

Direct assessment of hepatic mitochondrial oxidative and anaplerotic fluxes in humans using dynamic ^{13}C magnetic resonance spectroscopy

Douglas E. Befroy, Rachel J. Perry, Nimit Jain, Sylvie Dufour, Gary W. Cline, Jeff Trimmer, Julia Brosnan, Douglas L. Rothman, Kitt Falk Petersen and Gerald I. Shulman

Supplemental Information

Table S1. Morphological characteristics and intrahepatic lipid (IHL) content for the subjects participating in the study.

	n	Mean	SEM
Age (yr)	12	28.3	± 2.0
Height (m)	12	1.76	± 0.02
Weight (kg)	12	70.1	± 2.7
BMI (kg m^{-2})	12	22.7	± 0.5
IHL (%)	12	1.09	± 0.19

Figure S1. Representative Monte Carlo simulations and probability distribution analysis for the modeled rates of hepatic TCA cycle flux (V_{TCA}) and anaplerosis (V_{ANA}) for a single subject.

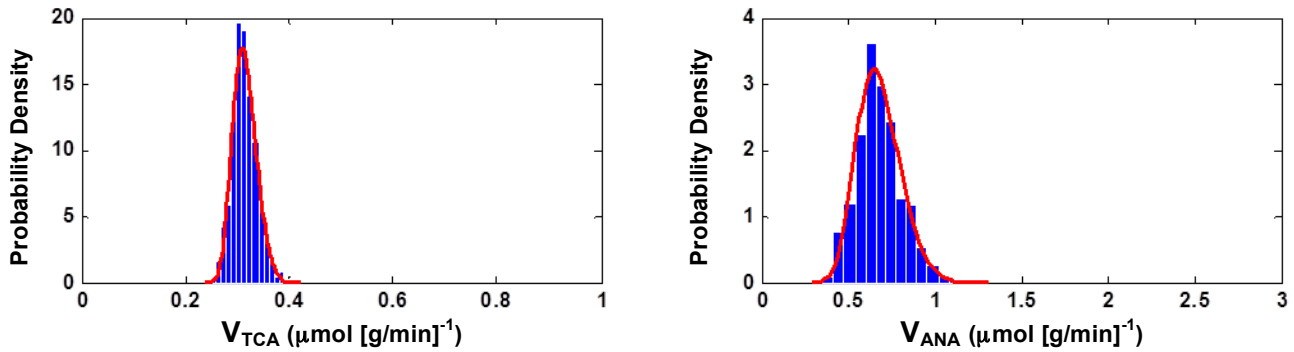
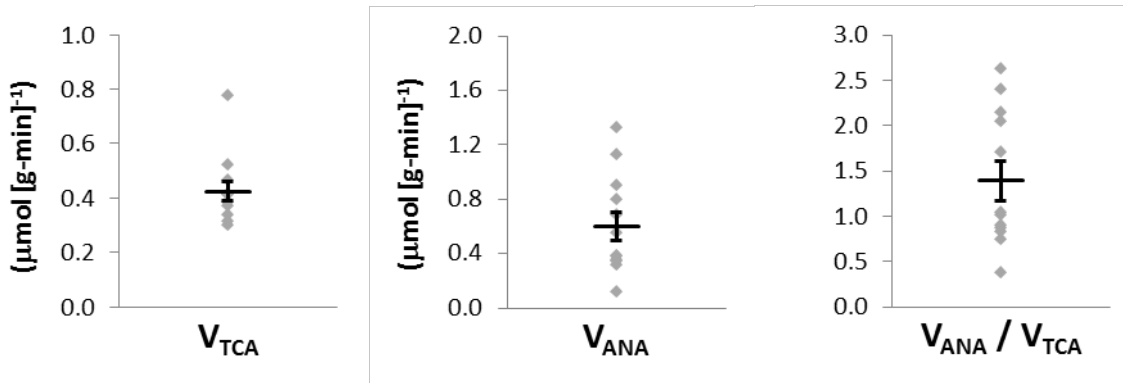


Figure S2. Scatter plots of V_{TCA} , V_{ANA} and V_{ANA}/V_{TCA} data for the individual subjects ($n = 12$, gray diamonds); the group mean (black line) and SEM of the data are superimposed.



Isotopic and mass balance differential equations used in the metabolic modeling analysis

$$\frac{dC_1AcCoA}{dt} = V_{DIL} \left(\frac{\text{unlabeled } \square FA}{FA} \right) + V_{AC} \left(\frac{C_1Acetate}{Acetate} \right) - V_{TCA} \left(\frac{C_1AcCoA}{AcCoA} \right)$$

$$\frac{dC_5Citrate}{dt} = V_{TCA} \left(\frac{C_1AcCoA}{AcCoA} \right) - V_{TCA} \left(\frac{C_5Citrate}{Citrate} \right)$$

$$\frac{dC_5\alpha KG}{dt} = V_{TCA} \left(\frac{C_5Citrate}{Citrate} \right) + V_X \left(\frac{C_5Glutamate}{Glutamate} \right) - [V_{TCA} + V_X] \left(\frac{C_5\alpha KG}{\alpha KG} \right)$$

$$\frac{dC_5Glutamate}{dt} = V_X \left(\frac{C_5\alpha KG}{\alpha KG} \right) - V_X \left(\frac{C_5Glutamate}{Glutamate} \right)$$

$$\frac{dC_4Malate}{dt} = \frac{V_{TCA}}{2} \left(\frac{C_5\alpha KG}{\alpha KG} \right) + \frac{V_{TCA}}{2} \left(\frac{\text{unlabeled } \square \alpha KG}{\alpha KG} \right) - V_{TCA} \left(\frac{C_4Malate}{Malate} \right)$$

$$\frac{dC_1Malate}{dt} = \frac{V_{TCA}}{2} \left(\frac{C_5\alpha KG}{\alpha KG} \right) + \frac{V_{TCA}}{2} \left(\frac{\text{unlabeled } \square \alpha KG}{\alpha KG} \right) - V_{TCA} \left(\frac{C_1Malate}{Malate} \right)$$

$$\frac{dC_4OAA}{dt} = V_{TCA} \left(\frac{C_4Malate}{Malate} \right) + V_{ANA} \left(\frac{*CO_2}{CO_2} \right) + V_X \left(\frac{C_4Aspartate}{Aspartate} \right) - (V_{TCA} + V_{ANA} + V_X + V_{FUM}) \left(\frac{C_4OAA}{OAA} \right) + V_{FUM} \left(\frac{C_1OAA}{OAA} \right)$$

$$\frac{dC_1OAA}{dt} = V_{TCA} \left(\frac{C_1Malate}{Malate} \right) + V_{ANA} \left(\frac{\text{unlabeled } \square Pyruvate}{Pyruvate} \right) + V_X \left(\frac{C_1Aspartate}{Aspartate} \right) - (V_{TCA} + V_{ANA} + V_X + V_{FUM}) \left(\frac{C_1OAA}{OAA} \right) + V_{FUM} \left(\frac{C_4OAA}{OAA} \right)$$

$$\frac{dC_4Aspartate}{dt} = V_X \left(\frac{C_4OAA}{OAA} \right) - V_X \left(\frac{C_4Aspartate}{Aspartate} \right)$$

$$\frac{dC_1Aspartate}{dt} = V_X \left(\frac{C_1OAA}{OAA} \right) - V_X \left(\frac{C_1Aspartate}{Aspartate} \right)$$

$$\frac{dC_1Citrate}{dt} = V_{TCA} \left(\frac{C_4OAA}{OAA} \right) - V_{TCA} \left(\frac{C_1Citrate}{Citrate} \right)$$

$$\frac{dC_6Citrate}{dt} = V_{TCA} \left(\frac{C_1OAA}{OAA} \right) - V_{TCA} \left(\frac{C_6Citrate}{Citrate} \right)$$

$$\frac{dC_1\alpha KG}{dt} = V_{TCA} \left(\frac{C_1Citrate}{Citrate} \right) + V_X \left(\frac{C_1Glutamate}{Glutamate} \right) - [V_{TCA} + V_X] \left(\frac{C_1\alpha KG}{\alpha KG} \right)$$

$$\frac{dC_1Glutamate}{dt} = V_X \left(\frac{C_1\alpha KG}{\alpha KG} \right) - V_X \left(\frac{C_1Glutamate}{Glutamate} \right)$$

$$V_{TCA} = V_{DIL} + V_{AC}$$

$$V_{DIL} = V_{PDH} + V_{FA}$$

$$V_{ANA} = V_{PEPCK} = V_{PC}$$

$$\left(\frac{*CO_2}{CO_2} \right) = \left(\frac{H *CO_3}{HCO_3} \right)$$

Methodological validation: animal experiments

To validate the methodological approaches described in this article, analogous experiments were performed *ex vivo* in rat liver. All experiments were performed in compliance with protocols approved by the Yale University Institutional Animal Care and Use Committee.

¹³C MRS assessment of hepatic TCA Cycle Flux

Adult (8-10 week), male *Sprague-Dawley* rats ($n = 34$) underwent a 2-step primed-continuous infusion of [$1-^{13}\text{C}$] acetate for varying durations up to 120 minutes [prime 1: $358 \mu\text{mol (kg-min)}^{-1} \times 5 \text{ min}$, prime 2: $178 \mu\text{mol (kg-min)}^{-1} \times 5 \text{ min}$, continuous: $130 \mu\text{mol (kg-min)}^{-1} \times 110 \text{ min}$]. Blood samples were drawn at regular intervals throughout the infusion protocol to assess plasma acetate concentration and [$1-^{13}\text{C}$] enrichment by gas chromatography-mass spectrometry (GC/MS). At the end of each infusion the liver was excised and immediately freeze-clamped with liquid nitrogen. The relative, positional ^{13}C -enrichments of glutamate were determined by ^{13}C -NMR of liver extracts at 500MHz; total ^{13}C -enrichment and glutamate concentration were determined by liquid-chromatography–mass-spectrometry–mass spectrometry (LC/MS/MS). Composite time courses of hepatic glutamate enrichment were fitted as individual points to the metabolic model of the TCA cycle as described for the human experiments in the **Online Methods**. TCA cycle flux is reported as the best fit \pm the SD of the fit.

Assessment of glucose turnover in vivo in awake rats

Rats ($n = 4$) were infused for 120min with [$3-^3\text{H}$] glucose using a 1-step primed-continuous protocol as described by Rosetti *et al*¹. Plasma samples were drawn at 100, 110 and 120 min, deproteinized with methanol, dried, and ^3H specific activity measured using a scintillation counter. Rates of endogenous glucose production were calculated at steady-state, according to the equations of Steele².

Contribution of pyruvate to gluconeogenesis and TCA cycle flux

The relative contributions of pyruvate to endogenous glucose production and the oxidation of pyruvate to the overall hepatic TCA cycle flux (V_{PDH}/V_{TCA}) were determined in rats infused with $3-^{13}\text{C}$ -lactate. Each animal was infused for 120 min with a 2-step primed-continuous protocol [prime1: $358 \mu\text{mol (kg-min)}^{-1} \times 5 \text{ min}$; prime2: $178 \mu\text{mol (kg-min)}^{-1} \times 5 \text{ min}$; continuous: $130 \mu\text{mol (kg-min)}^{-1} \times 115 \text{ min}$]. At the end of the experiment the liver was excised and immediately freeze-clamped. Total pyruvate and glutamate enrichments were determined by LC/MS, and glucose enrichments by GC/MS, of liver extracts; positional enrichments were assigned by ^{13}C NMR at 500 MHz. The contribution of pyruvate to gluconeogenesis was determined from the sum of the enrichments of $\text{C}_1\text{-C}_2\text{-C}_5\text{-C}_6$ -glucose relative to $\text{C}_2\text{-C}_3$ -glutamate. The ratio of PDH to TCA cycle flux was calculated assuming $V_{PDH}/V_{TCA} = (\text{C}_4^*\text{Glu})/(\text{C}_3^*\text{Pyr})$. The relative anaplerotic to TCA cycle flux was estimated assuming $V_{ANA}/V_{TCA} = (\text{C}_4^*\text{Glu} - \text{C}_2^*\text{Glu})/(\text{C}_3^*\text{Glu} + \text{C}_2^*\text{Glu} - \text{C}_3^*\text{Pyr} + \text{C}_2^*\text{Pyr})$. C_x^* metabolite denotes the positional ^{13}C enrichment of a particular metabolite.

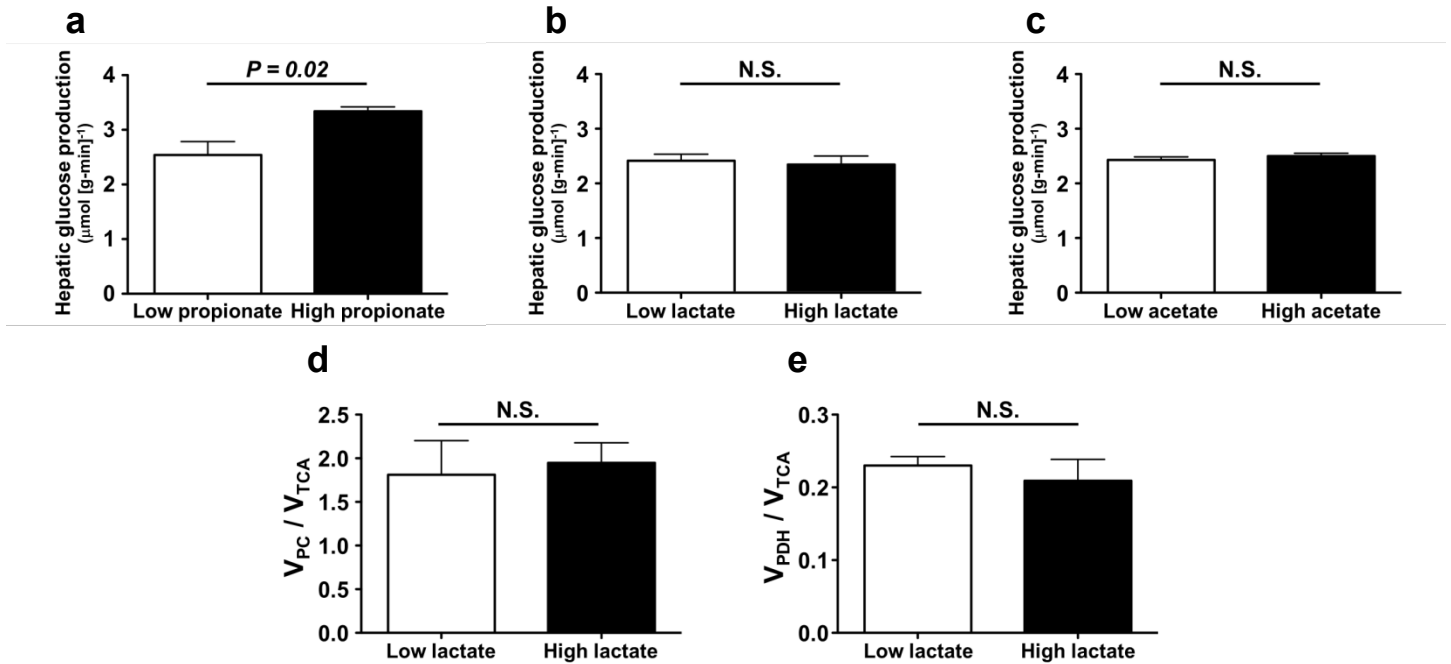
Effects of exogenous propionate

To determine the effects of the provision of exogenous propionate on hepatic metabolism, rats were given an intravenous infusion of propionate at either a low [333 $\mu\text{mol kg}(\text{body-weight})^{-1}$ over 120 min, $n = 3$] or a high dose [666 $\mu\text{mol kg}(\text{body-weight})^{-1}$ over 120 min, $n = 4$] with concurrent assessment of glucose turnover. In order to avoid interference with the ^{13}C label derived from 1- ^{13}C acetate, [3- ^3H] glucose was infused at rates of 0.05 $\mu\text{Ci min}^{-1}$ for 120 min to assess rates of glucose turnover. Plasma samples were taken at steady state (100-120 min) for assessment of glucose ^3H specific activity and rates of glucose turnover were calculated as previously described³. The sample size was chosen to detect ~20% differences between the groups, based on the coefficient of variation of previously reported data using this technique^{4,5}.

Table S2. Steady-state positional ^{13}C -enrichments of liver glutamate, pyruvate, and glucose in rats ($n = 4$) undergoing a 3- ^{13}C lactate infusion. Endogenous glucose production was determined using the [6,6- $^2\text{H}_2$] glucose turnover method. Estimates of the relative contributions of pyruvate to gluconeogenesis, pyruvate flux into the TCA cycle (V_{PDH}/V_{TCA}) and the overall TCA cycle flux.

	Mean	SEM
C₂+C₃-Pyruvate APE (%)	20.3	± 1.8
C₂-Glutamate APE (%)	8.1	± 0.1
C₃-Glutamate APE (%)	7.3	± 0.3
C₄-Glutamate APE (%)	0.5	± 0.1
C₁-Glucose APE (%)	5.2	± 0.9
C₂-Glucose APE (%)	3.2	± 0.1
C₅-Glucose APE (%)	3.4	± 0.3
C₆-Glucose APE (%)	4.6	± 0.6
endogenous glucose production ($\mu\text{mol [g-liver-min]}^{-1}$) 3-carbon units	2.4	± 0.1
contribution of pyruvate to gluconeogenesis (%)	93.3	± 1.3
V_{PDH}/V_{TCA}	0.16	± 0.1
V_{ANA}/V_{TCA}	1.9	± 0.4
Estimated V_{TCA} ($\mu\text{mol [g-liver-min]}^{-1}$) 2-carbon units	1.4	± 0.4

Figure S3. Effect of substrate provision on relative hepatic metabolic fluxes. High dose reflects double the infusion rate described in the supplemental methods (a) Hepatic glucose production in rats infused with low ($n = 3$) or high dose propionate ($n = 4$). (b) Hepatic glucose production in rats infused with low ($n = 3$) or high dose lactate ($n = 3$). (c) Hepatic glucose production in rats infused with low ($n = 3$) or high dose acetate ($n = 3$). (d) V_{PC}/V_{TCA} in rats infused with low or high dose 3- ^{13}C lactate. (e) V_{PDH}/V_{TCA} in rats infused with low or high dose 3- ^{13}C lactate. Statistically significant differences between the low dose and high dose groups subjects were detected by using an unpaired 2-tailed student's t test. A P value of < 0.05 was considered statistically significant; N.S. indicates non-significant.



References

1. Rossetti, L., *et al.* Mechanism by which hyperglycemia inhibits hepatic glucose production in conscious rats. Implications for the pathophysiology of fasting hyperglycemia in diabetes. *J Clin Invest* **92**, 1126-1134 (1993).
2. Steele, R. Influences of glucose loading and of injected insulin on hepatic glucose output. *Ann N Y Acad Sci* **82**, 420-430 (1959).
3. Jornayvaz, F.R., *et al.* Thyroid hormone receptor-alpha gene knockout mice are protected from diet-induced hepatic insulin resistance. *Endocrinology* **153**, 583-591 (2012).
4. Jin, E.S., *et al.* Glucose production, gluconeogenesis, and hepatic tricarboxylic acid cycle fluxes measured by nuclear magnetic resonance analysis of a single glucose derivative. *Anal Biochem* **327**, 149-155 (2004).
5. Jones, J.G., *et al.* Measurement of gluconeogenesis and pyruvate recycling in the rat liver: a simple analysis of glucose and glutamate isotopomers during metabolism of [1,2,3-(^{13}C)]propionate. *FEBS Lett* **412**, 131-137 (1997).